CHEMISTRY OF MATERIALS
Cite This: Chem. Mater. 2018, 30, 6769−6776
Article
pubs.acs.org/cm

Deposition and Stripping Behavior of Lithium Metal in Electrochemical System: Continuum Mechanics Study

Gabin Yoon,[†,‡] Sehwan Moon,[†] Gerbrand Ceder,[§,∥] and Kisuk Kang*[,†,‡]

[†]Department of Materials Science and Engineering, Research Institute of Advanced Materials (RIAM), Seoul National University, 1 Gwanak-ro, Gwanak-gu, Seoul 08826, Republic of Korea

[‡]Center for Nanoparticle Research, Institute for Basic Science (IBS), Seoul National University, 1 Gwanak-ro, Gwanak-gu, Seoul 08826, Republic of Korea

[§]Department of Materials Science and Engineering, University of California—Berkeley, Berkeley, California 94720, United States

[∥]Materials Sciences Division, Lawrence Berkeley National Laboratory, Berkeley, California 94720, United States

Supporting Information

ABSTRACT: Metallic lithium (Li) is a promising anode candidate for high-energy-density rechargeable batteries because of its low redox potential and high theoretical capacity. However, its practical application is not imminent because of issues related to the dendritic growth of Li metal with repeated battery operation, which presents a serious safety concern. Herein, various aspects of the electrochemical deposition and stripping of Li metal are investigated with consideration of the reaction rate/current density, electrode morphology, and solid electrolyte interphase (SEI) layer properties to understand the conditions inducing abnormal Li growth. It is demonstrated that the irregular (i.e., filamentary or dendritic) growth of Li metal mostly originates from local perturbation of the surface current density, which stems from surface irregularities arising from the morphology, defective nature of the SEI, and relative asymmetry in the deposition/stripping rates. Importantly, we find that the use of a stripping rate of Li metal that is slower than the deposition rate seriously aggravates the formation of disconnected Li debris from the irregularly grown Li metal. This finding challenges the conventional belief that high-rate stripping/plating of Li in an electrochemical cell generally results in more rapid cell failure because of the faster growth of Li metal dendrites.

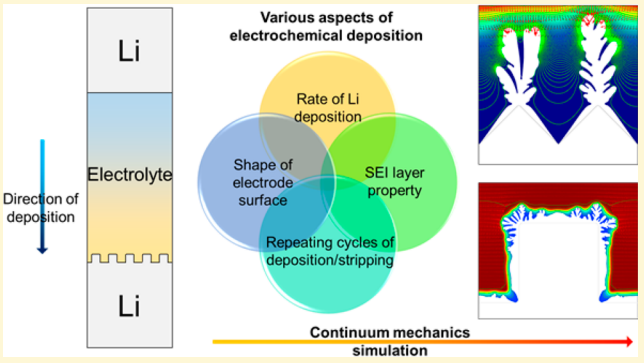

INTRODUCTION

The use of Li metal as an electrode in rechargeable batteries offers an unparalleled opportunity to boost the energy density of current lithium-ion batteries, as Li metal is capable of delivering the largest theoretical capacity (~3860 mAh g^{-1}) at the lowest redox potential (−3.04 V vs standard hydrogen electrode) of anode materials known to date.[1,2] However, the practical application of a Li metal anode remains far from realization because of issues arising from the dendritic growth of Li metal during electrochemical cycling, which raise serious safety concerns.[3−7] For instance, irregularly grown Li metal such as filaments on the anode or Li metal debris detached from the electrode can penetrate the separator and contact the cathode, resulting in an internal short circuit and thermal runaway. In addition, repeating the formation and removal of Li dendrites inevitably exposes a fresh surface of Li metal, which constantly consumes the electrolyte to form an unusually thick solid electrolyte interphase (SEI) layer on the electrode.[8,9] These undesirable phenomena continuously deteriorate the Coulombic efficiency, causing premature cell failure.

Several strategies have been adopted experimentally to address these issues. One widely used approach is the introduction of a mechanically robust layer at the surface to physically suppress the uncontrolled growth of Li dendrites.[10−20] Various physical coatings such as Al_2O_3, Li_3PO_4, solid Li ion conductors, h-BN, and different types of carbon have been used as a protection layer for the Li metal surface, resulting in some improvements.[13−19] Electrolyte additives such as fluoroethylene carbonate and $LiNO_3$ have also been adopted to induce the formation of a dense and mechanically stable SEI layer to protect the Li surface.[11,12] Alternatively, attempts have been made to control the flux of Li ions near the electrode surface. The addition of Li halide salts was successfully demonstrated to selectively enhance Li ion transport at the interface of the electrode, stabilizing the electrodeposition.[20,21] Cs ions dissolved in the electrolyte could more evenly distribute the flux of Li ions near the Li

Received: June 21, 2018
Revised: September 3, 2018
Published: September 11, 2018

DOI: 10.1021/acs.chemmater.8b02623
Chem. Mater. 2018, 30, 6769−6776

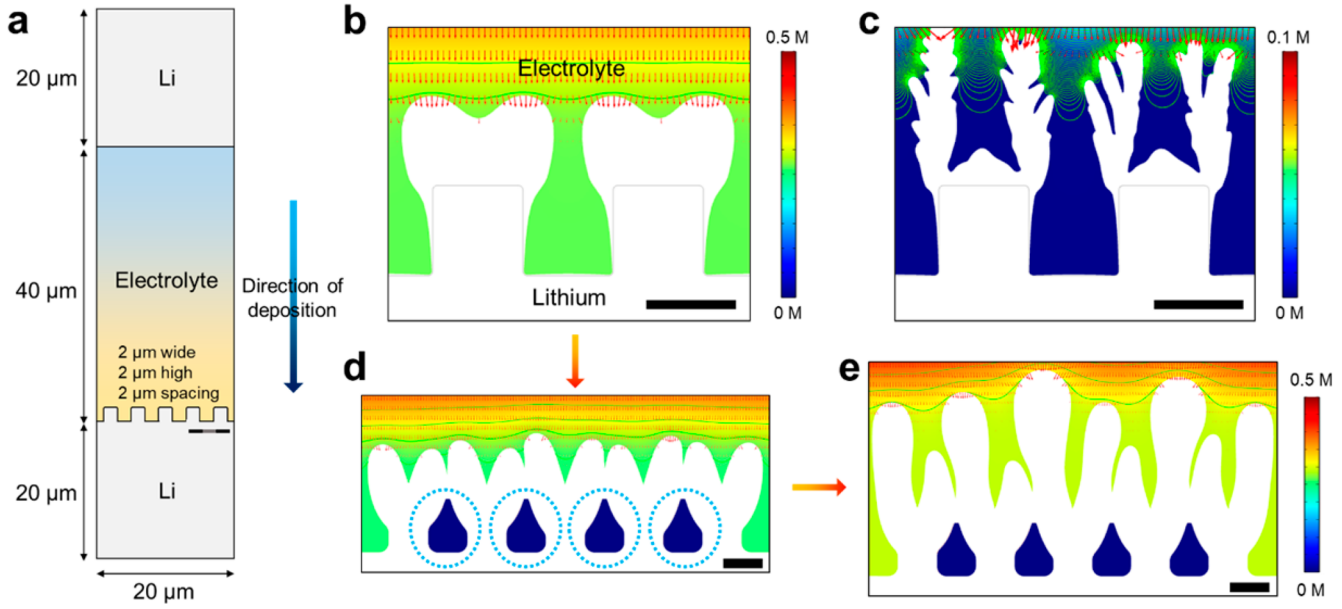

Figure 1. Evolution of Li deposits for different deposition rates. (a) Reference model used for simulations. Geometry after initial deposition at (b) slow and (c) fast deposition rates. The gray lines represent the initial geometry before deposition. (d) Expected shape after continuous deposition at slow rate. The dotted circles represent pores that could be generated after physical contact between deposits. (e) Geometry after further deposition from (d). Deposits from neighboring bumps will meet and eventually form a mossy-like shape, whereas the high-rate condition yields vertical growth of Li with many branches, forming a needle-like shape. The scale bars are 2-μm long. The utilization of Li is identical in (b) and (c). The contour levels of the potential are displayed every 2.5 meV.

metal surface because of the resulting electrostatic repulsive force.[22] The use of vertically aligned Cu microchannels exhibited the enhanced cycling and rate performance of Li deposition and stripping due to the regulation of the current density distributions along the microchannel walls.[23] Although these treatments were partly successful in enhancing the stability of the Li metal anode, as confirmed by the prolonged cycle life, the thin protection layers were eventually cracked by the morphological growth of Li metal. In addition, attempts to control the local Li flux near the electrode surface could not ultimately suppress the propagation of dendrites, especially at high current rates and large utilization levels, leading to cell failure. Moreover, the intrinsic inhibition of dendritic growth for extended cycles under practical operation conditions has yet to be achieved.

In this respect, it is important to revisit the fundamentals of Li electrodeposition and stripping in an electrochemical system. Indeed, some theoretical studies have aimed to understand the basic Li deposition behavior. Rosso and Chazalviel et al. investigated the initial nucleation and growth of Li dendrites using an analytical model of the system.[24−27] By interpreting the evolution of the ion concentrations in a simplified uniform one-dimensional model, they suggested that the ion concentration at the electrode would fall to zero after a certain time, called Sand's time (referring to the original work by Sand[28]), after which the potential on the electrode surface would start to diverge. In addition, it was claimed that at Sand's time, the dendrites begin to appear to escape the instability of the system.[26] Later, optical microscopy analysis revealed that the dendritic growth of Li metal occurred after Sand's time.[29] Although these works regarding Sand's time successfully describe the initiation of Li dendrites and offer important insight into the conditions of abnormal growth, a comprehensive understanding of the effects of the practical conditions of Li deposition and stripping in the electrochemical systems (such as the applied current rates or the history of the current rates and surface properties of the electrode) on the formation of the initial morphology, growth behavior, and propagation of the Li dendrites remains lacking. A systematic understanding of the Li growth mechanisms and behaviors with respect to the various experimental conditions would potentially enable practical application of Li metal batteries.

In this work, we investigate the key factors affecting electrochemical Li deposition and stripping by performing continuum mechanics simulations to monitor the evolution of the Li morphology on the electrode. The rate of Li deposition/stripping, shape of the electrode surface, conductivity, and uniformity of the SEI layer, and effect of the current density history on Li deposition/stripping were studied as representative practical parameters affecting the geometry of Li deposits. Our findings here not only elucidate the quantitative Li growth behaviors under various applied electrochemical conditions but also provide insight into the possible origins of different shapes of Li deposits and the formation of electrically isolated Li metal debris.

METHODS

All the simulations on lithium electrodeposition were conducted using the electrodeposition module with tertiary current distribution and Nernst−Planck interface in COMSOL Multiphysics.[30] The behaviors of the charged species in an electrolyte were treated using the Nernst−Planck equation with the assumption of charge conservation described below:

$$\boldsymbol{N_i} = -\boldsymbol{D_i}\nabla c_i - z_i u_i F c_i \nabla \varphi_i$$

$$\sum_i z_i c_i = 0$$

Here, $\boldsymbol{N}_i$ is the flux of the ionic species i, $\boldsymbol{D}_i$ is the diffusion coefficient, c_i is the concentration, z_i is the valence, u_i is the mobility, φ_i is the

DOI: 10.1021/acs.chemmater.8b02623
Chem. Mater. 2018, 30, 6769−6776

electrolyte potential of each species, and F is the Faraday constant. The contribution of convection to the flux was neglected. The material balances were conserved using the following mass conservation law:

$$\frac{\partial c_i}{\partial t} + \nabla \times \mathbf{N}_i = 0$$

The reaction kinetics at the electrode surface were described using the concentration-dependent Butler−Volmer equation:.

$$i = i_0\left(C_R \exp\left(\frac{\alpha_a F\eta}{RT}\right) - C_O\left(\frac{-\alpha_c F\eta}{RT}\right)\right)$$

where i_0 is the exchange current density; C_R and C_O are the dimensionless concentrations of the reduced and oxidized species, respectively; α_a and α_c are the anodic and cathodic charge transfer coefficients, respectively; η is the activation overpotential; R is the gas constant; and T is the temperature. The resulting electrodeposition was assumed to occur in the normal direction to the boundary with a velocity v:

$$v = \frac{i}{nF}\frac{M}{\rho}$$

where M and ρ are the molar mass and density of Li, respectively.

The equations above govern the ion transport behavior in the electrolyte and the electrodeposition reaction at the electrode/electrolyte surface. All the other boundaries were treated as insulating, as described by the following equation:

$$\boldsymbol{N}_i \times \boldsymbol{n} = 0$$

Here, $\boldsymbol{n}$ represents the vector normal to each boundary.

Each charge transfer coefficient was set to 0.5 and the temperature was fixed at 300 K in all the simulations. The initial Li ion diffusion coefficient in the electrolyte was set to 7.5×10^{-11} m^2 s^{-1}, which is close to the values for conventional electrolytes.[31] We used an initial Li ion concentration of 1 M, and the overpotential for Li deposition was kept in the range of 0.4−0.7 V to control the rates of the deposition and stripping reaction. The other input parameters were systematically controlled to monitor the effect of variables, such as the rate of Li deposition, shape of the electrode surface, SEI layer conductivity and uniformity, and repeating cycle of Li deposition and stripping. To elucidate how the specific variables in electrochemical cells affect the Li metal evolution on the electrode, the conditions were independently imposed in the following simulations.

RESULTS AND DISCUSSION

The standard model used for the overall simulation is described in Figure 1a. Because a reaction on an ideally flat and clean surface necessarily results in uniform and monotonous deposition, we intentionally built a surface with reference bumps to induce irregularity of the ion flux, which better reflects the general experimental conditions. Using this model as an initial geometry, the evolution of Li deposition behavior was comparatively examined under diverse conditions.

Effect of Deposition Rate on Li Growth Behavior. The initial deposition on the electrode with the reference bumps ($2 \times 2 \times 2$ μm^3) was performed using a relatively slow rate and is described as a reference in Figure 1b. In the conditions of slow deposition and stripping, we applied the overpotential of 0.4 V to the system, while a higher overpotential of 0.7 V was applied for fast deposition and stripping. In the figure, the background color indicates the local Li ion concentration in the electrolyte, the green lines are equipotential lines, and the red arrows represent the intensity and direction of the Li ionic current density. It is apparent that the Li deposition was locally concentrated at the corners of the surface bumps. More in-depth examination of this initial stage (see Supporting Information, SI, Movie M1 for time-dependent geometry evolution) revealed that the ionic current densities were higher around the corners, making them preferential deposition sites. However, the Li ion concentration at the corner did not drop to zero at the surface because of the relatively low current density, and the Li deposit was rather spherical, covering the corner. However, when a high current rate was applied, as shown in Figure 1c, the Li deposition occurred much more vertically toward the counter electrode, which was accompanied by the formation of a number of branches. The equipotential lines (green lines) shown in Figure 1c are significantly denser than those in Figure 1b around the corner (or the forefront of the Li branches after the growth), indicating that a strong electric field was locally developed, inducing a high flux of the Li ionic current. For this high-rate deposition, even a small inhomogeneity would induce a non-negligible disturbance of the current distribution and a correspondingly high localized ionic current density, leading to directional growth toward the counter electrode as well as the formation of branches (SI Movie M2). Another significant difference from the low-rate condition was the depletion of the Li ion concentration to zero near the surface of the electrode, shown by the dark blue color in Figure 1c. This depletion of Li ions at the surface and simultaneous observation of directional and branching growth of Li metal agrees well with the early theoretical work of Chazalviel.[26]

Even though the initial growth under the slow deposition conditions (Figure 1b) was less directional, the continuing deposition under this condition would result in physical contact among neighboring deposits on the side, as shown in Figure 1d. It is noteworthy that the merging of the growing deposits inevitably involves the formation of a porous structure underneath the growing forefront of the Li metal, as indicated by the dotted circles in the figure. Even if the electrodeposition proceeded further, then the inner areas with the dotted circles would not participate in the deposition reaction and would not be filled in, as illustrated in Figure 1e. However, further deposition occurs mostly at the forefront of the Li deposits, giving the neighboring deposits a chance to grow and merge again. Repeating this process would lead to an overall porous geometry, resembling the mossy shape of Li metal deposits observed experimentally.[29]

On the basis of the results for different current rates, it can be concluded that the initial deposition occurs primarily at deposition seeds where the equipotential lines are densely distributed for geometric reasons, followed by their evolution into different forms depending on the current rate. The slow deposition condition does not induce severe preferential deposition at regions of minor irregularity, leading to less directional growth; however, a porous structure eventually develops because of the initial uneven geometry. In contrast, at high current rates, preferential deposition with the formation of a number of branches is easily triggered even by a small inhomogeneity, and the complete depletion of Li ions is often observed at the surface of the electrode, leading to unidirectional and dendritic growth of Li metal.

Effect of Surface Geometry on Li Growth Behavior. As local geometric irregularities were observed to act as seeds for the abnormal growth of Li, we attempted to understand the effect of the initial surface geometry using different surface shapes during Li deposition. Triangular- and circular-shaped bumps were compared with the previous case of square-shaped

DOI: 10.1021/acs.chemmater.8b02623
Chem. Mater. 2018, 30, 6769−6776

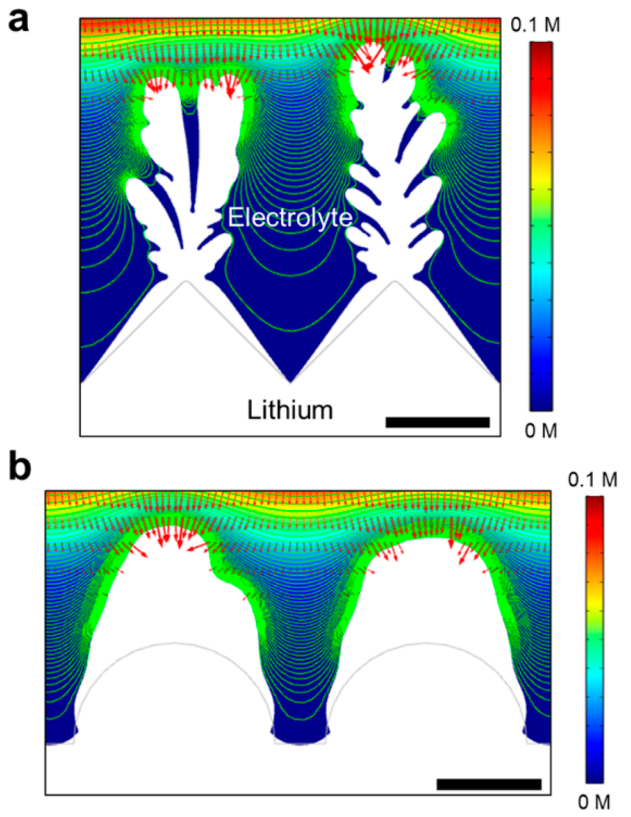

Figure 2. Evolution of Li deposits starting from an initial surface geometry with (a) triangular and (b) circular bumps. The gray lines represent the initial geometry before deposition, and the scale bars are 2-μm long. The utilization of Li is identical in (a) and (b), and the contour levels of potential are displayed every 2.5 meV.

bumps, as shown in SI Figure S1. All the other parameters were the same as those for Figure 1c. Figure 2a shows the final shape of the Li deposits starting from the surface with triangular bumps. Dendritic growth appeared to occur from the exposed corner of the triangular bump. Because of the densely populated equipotential lines around the sharp corners, the preferential depositions led to extremely directional and branching growth of Li metal (SI Movie M3). Notably, the final length of the dendritic deposits was much longer than that observed in Figure 1c, implying that the shape and number of initial seeds are important factors in determining the length and size of dendrites in the Li deposition. However, the deposition on the surface with smooth circular bumps yielded quite uniform and dense growth, as shown in Figure 2b. The lack of irregular areas on the surface resulted in well-distributed current along the smooth surface with a large area without current concentrations at certain points, which resulted in a shorter length of deposits, as shown in SI Movie M4. However, if the deposition proceeds further and the surface irregularities are accumulated, then points with high local current density are generated accompanied by the evolution of filamentary growth with branches. Fast deposition will also accelerate the onset of the branching growth, therefore, the irregular deposition can be eventually observed at the smooth surface after an extended deposition. Nevertheless, a smoother initial surface delays the onset of branching, providing more space for the dense and uniform deposition of Li within a certain utilization level.

Effect of SEI Layer Properties on Li Growth Behavior.

In the previous sections, we used simple models consisting of Li metal electrodes and an electrolyte for the electrodeposition without the presence of additional phases on the interface. However, it is widely known that a SEI layer is typically generated at the surface of electrodes because of the decomposition of the electrolyte, and this layer plays a crucial role in battery operation.[1,32] Typical SEI layers in practical cells exhibit low electrical conductivities and reasonably high Li ion conductivities; thus, they prevent further electrochemical decomposition of the electrolyte while allowing the passage of Li ions. The salts, solvent, and electrode materials used in the cell significantly affect the properties of the SEI layers such as the constituting elements, electrical conductivity, and Li ion diffusivity, thereby affecting the performance of the electrochemical cell. To account for this SEI layer, we introduced an artificial layer at the surface of the electrode with different transport properties, as shown in SI Figure S2. A 200 nm-thick interphase layer with a Li ion diffusivity 100-times-lower than that of the electrolyte was adopted as a reference model in the calculations, considering that the Li ion diffusivity in a solid medium (e.g., constituents of SEI or solid-state electrolyte) is generally orders of magnitude lower than that in liquid electrolytes.[33]

Figure 3a depicts the Li deposition behavior with the presence of the SEI layer on the electrode. The most notable difference compared with the previous results is that the Li growth is much more dendritic, indicating that the tendency for preferential deposition is far greater under this condition. It should be noted that Figure 3a shows Li deposits deposited at a relatively lower deposition rate (applied overpotential of 0.5 V) than that used for the previous cases (0.7 V) because the use of the same deposition rate as that in Figures 1c and 2 yielded severe branching growth even from the initial stage. The dramatic color change near the surface of the electrode in Figure 3a provides a clue about the cause of this phenomenon, as the Li ion concentration was much higher outside the SEI layer and rapidly decreased within the SEI layer upon approaching the electrode surface. Because the transport of Li ions is comparatively hampered within the SEI layer, the supply of Li ions to the electrode surface was not sufficiently rapid for the incessant reaction, inducing the significant concentration gradient within the SEI layer. The right panel in Figure 3a shows the Li ion concentration along the vertical line across the interface, which also confirms the abrupt decrease of the Li ion concentration in the SEI layer. Under this severe concentration gradient condition, even a small protrusion of Li metal would cause significant distortion of the equipotential lines of the ionic flux, resulting in a high local current density near the protrusion and triggering dendritic growth. The dendritic growth of Li metal not only occurred near the original corner region but also in other areas, as shown in Figure 3a, indicating that minor protrusions could also induce dendritic growth even at slow current rates.

Since the SEI layer in the simulation was simply described by presenting a surface layer with reduced ionic diffusivity compared with that of the electrolyte, the diffusion in the SEI layer retains a characteristic bi-ionic conducting property of the conventional liquid electrolyte, where both Li ion and anion are mobile. However, considering that typical SEI layer is mostly composed of inorganic compounds, its single-ionic conducting characteristic should be carefully examined. In this regard, we conducted a simulation using the SEI layer with

DOI: 10.1021/acs.chemmater.8b02623
Chem. Mater. 2018, 30, 6769−6776

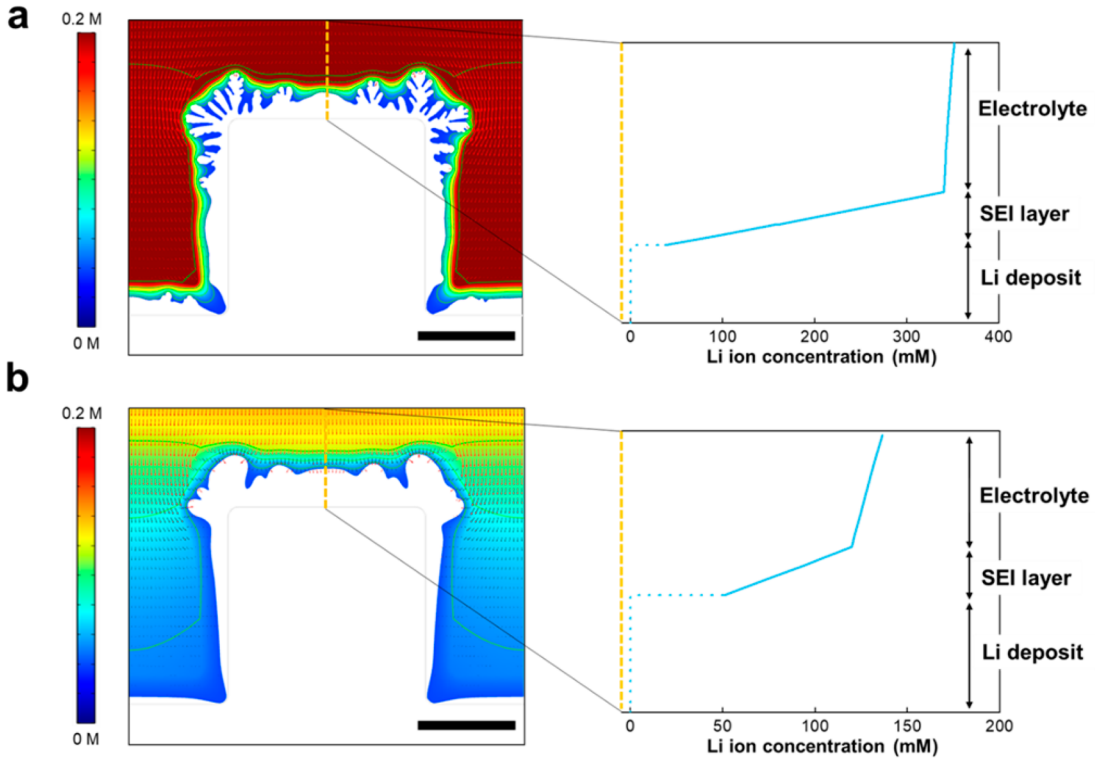

Figure 3. Evolution of Li deposits with the presence of a 200 nm-thick surface SEI layer. The Li ion concentration profile along the yellow dotted line is also shown. The Li ion conductivity of the layer was set to (a) 100 times and (b) 10 times lower than that of the electrolyte. The gray lines represent the initial geometry before deposition, and the scale bars are 1-μm long. The utilization of Li is identical in (a) and (b), and the contour levels of potential in (a) and (b) are displayed every 10 meV.

single-ionic conducting nature, while maintaining all other conditions identical. SI Figure S3 compares the Li ion and the potential profile in the electrolyte region, when single and bi-ionic conducting SEI layer is adopted, respectively. Since the anions are immobile in single-ionic conductor, Li ion concentration gradient is not observed in the SEI as shown in SI Figure S3a. In addition, the potential gradient becomes linear, indicating that the Ohmic drop in the SEI is the sole source inducing the potential profile. Alternatively, the potential gradient is parabolic in bi-ionic conducting SEI, implying that both Ohmic drop and the Li ion concentration gradient affect the potential profile. This difference leads to slightly less severe branching growth of Li metal with the single-ionic SEI layer. Nevertheless, the branching growth is still observed, because sluggish SEI acts as high resistance regardless of its conducting nature, resulting in steep Ohmic drop in SEI layer, as described in SI Figure S4. The high local current density is thus induced at the surface, and the generation of minor protrusions leads to the branching growth as discussed in previous sections.

Our observations hitherto consistently suggest that the high local current density at the surface induced by the steep potential gradient leads to the unwanted branching growth of Li. Nevertheless, the findings above propose that the potential gradient near the surface can be regulated using the single-ionic conductor SEI layer, since it diminishes the effect of the Li concentration gradient. The impact would be more dramatic for ideal solid electrolytes with purely single-ion conducting characteristics, particularly for the case when the Li metal and solid electrolytes are stabilized without the formation of SEI layer. In this case, as described in SI Figure S5, the Ohmic drop is the sole source determining the potential profile in the electrolyte region. It would result in the linear potential gradient near the solid electrolyte interface without the Li ion concentration gradient, thus much smoother Li metal growth can be achieved (SI Figure S6). Moreover, it implies that the thickness of the single ionic conductor (or solid electrolyte) could be an important design criteria for the uniform Li deposition, since the linear potential gradient near the surface would be governed by the thickness of the electrolyte with a given applied voltage. The observations in Figure 3a imply that the presence of the SEI layer can substantially affect the deposition behavior and trigger unwanted morphological Li metal growth because of the inferior ionic transport that induces severe Li concentration gradients within the SEI layer. In this respect, we further examined the effect of properties of the SEI layer, such as the Li ion diffusivity and layer thickness, on Li metal growth on the electrode. Figure 3b shows the morphological evolution of the Li deposits when an SEI layer with higher Li ion diffusivity (10 times faster than that of the SEI layer in Figure 3a) was adopted. Because the Li ion transport through the SEI layer was faster, the bottleneck in the supply of Li ions toward the electrode surface became less problematic. Therefore, the concentration gradient within the SEI layer was less abrupt, as shown in the right panel of the figure, and the resulting geometry displayed much smoother growth compared with the previous case. Moreover, reduction of the SEI thickness from 200 to 50 nm resulted in less severe dendritic growth of Li on the surface (SI Figure S7), indicating the importance of the Li ion transport kinetics through the SEI layer in the formation of Li dendrites. The diffusion length of Li ions in the SEI layer is thought to be smaller for a thinner SEI layer; thus, the supply of Li ions to the electrode surface

DOI: 10.1021/acs.chemmater.8b02623
Chem. Mater. 2018, 30, 6769−6776

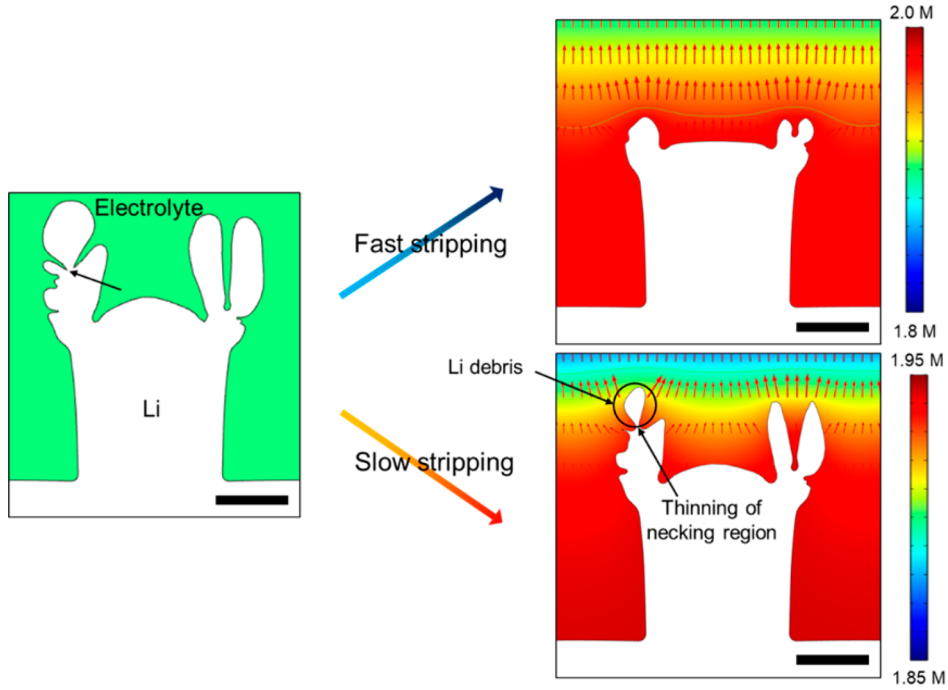

Figure 4. Li stripping behavior from irregular deposit. Dead Li formation is shown at the narrow point (black arrow) for the slow stripping condition. Complete stripping was not achieved because of the failure of the solution converge, presumably arising from the dynamic generation of singular points during the stripping reaction. The scale bars are 1-μm long.

becomes effectively facile, suppressing the buildup of the concentration gradient within the SEI layer.

These results imply that inducing the formation of a highly conductive and thin SEI layer on the electrode is of critical importance in tailoring the Li growth. The formation of an ideal SEI layer with Li ion diffusivity equivalent to that in the liquid electrolyte would prevent the development of an undesirably large concentration gradient within the SEI layer, inhibiting the local high current density near any possible protrusion. We note, however, that this argument is only valid under the assumption that the reduction process from Li ion to metallic Li is sufficiently fast on the electrode surface and not rate-limiting. In addition, our current model system does not account for certain properties of the SEI layer, such as its mixed-phase nature and mechanical properties and the dynamic process of rupture and reformation at its surface. Nevertheless, we believe that the interplay between the Li ion transport properties in the SEI layer and the evolution of the dendrites observed in this simple system can be applied to the local evolution of Li dendrites. Because SEI layers observed in experiments are often irregular in terms of thickness and conductivity because of the reasons described above, the local SEI region with sluggish Li ion transport is expected to be more vulnerable to dendritic growth, serving as the weakest link, according to our model studies. This speculation of nonuniform Li growth is consistent with previous work showing that the nonhomogenous nature of SEI layers is more prone to trigger the irregular and dendritic growth of Li metal deposits.[34]

Consequences of Repeated Cycles of Deposition and Stripping. Thus far, we have attempted to investigate the conditions that can trigger dendritic growth of Li metal during deposition as well as the influencing factors. However, unlike in typical metal electrodeposition processes, practical batteries are operated for thousands of charge and discharge cycles, involving the same number of repeated deposition and stripping processes. Therefore, it is of importance to probe the progressive effects of the cycles of deposition and stripping on the Li growth behavior, particularly when each deposition and stripping condition begins to deviate from the given initial conditions. As a representative case, we applied a reverse bias with different stripping rates for the Li deposits obtained after a single deposition step and comparatively monitored the morphological evolutions.

Figure 4 shows the evolutions of the geometry of Li metal for two different stripping conditions (right panels) starting from the Li deposit deposited at a fast rate (left panel). When the stripping process was performed at a similarly fast rate as the deposition, the morphology returned to the initial geometry with high reversibility (no side reactions that could affect the nature of the electrode/interface/electrolyte during the cycles were considered in the calculations). This result was observed because the stripping reactions were the most active at the corners or at points with large curvature, where the equipotential lines were densely concentrated, as previously discussed for electrodeposition. This preferential stripping therefore resulted in the stripping direction toward the reduction of curved points, which is simply the reverse process of the deposition and induced the recovery of the smooth surface. However, at a relatively low current rate, isotropic stripping occurred uniformly throughout the Li deposits. Although the uniform process was desirable during the deposition, stripping under this condition can induce highly curved points in regions with irregular surfaces in the deposits, as illustrated in Figure 4. In particular, isotropic thinning around the necking region (as indicated by the black arrows) eventually led to the separation of a fragment of Li deposits from the bulk electrode, producing Li debris. To confirm that this thinning under slow stripping conditions causes the formation of Li debris from the necking regions, we artificially

DOI: 10.1021/acs.chemmater.8b02623
Chem. Mater. 2018, 30, 6769−6776

built a model containing similar regions and performed a stripping simulation. SI Figure S8 confirms that analogous behavior was consistently displayed. This phenomenon, known as the formation of "dead Li", has been observed in many experiments and has been blamed for the severe degradation of cycle stability and internal electrical shortage.[35,36] Our experimental results shown in Figure 4 and SI Figure S8 clearly demonstrate that the slow stripping of Li deposits with irregular shapes, which are often formed after deposition at a fast rate, easily contributes to the formation of dead Li. This finding implies that in a practical rechargeable battery, the use of a different rate of charge and discharge within a cycle would pose a higher risk for the formation of Li debris. Moreover, considering that the effective current rates applied to the electrode may change as a result of side reactions, which can cause the loss of the active electrode parts, similar issues may arise even in batteries operating using a constant charge and discharge current rate and may be aggravated with prolonged cycles.

SUMMARY

In this work, we investigated the deposition and stripping behavior of Li metal in an electrochemical cell considering various experimental conditions such as the applied current rates, initial surface morphology, nature of the SEI layer, and cycling process of deposition and stripping. Our findings confirmed that the preferential Li growth occurs because of the disturbance of the local current density resulting from the presence of irregular surface properties. In addition, the tendency of preferential growth was particularly promoted for high deposition rates because of the densely populated equipotential lines around the irregular surfaces. The presence of a SEI layer was shown to generally promote the abnormal growth of Li deposits even from minor protrusions. The nature of SEI layers with relatively sluggish ionic transport properties compared with those of a liquid electrolyte induced severe ionic concentration gradients near the electrode surface, indicating the importance of engineering of the SEI to inhibit abnormal Li growth. Finally, it was demonstrated that the history of the deposition/stripping processes could sensitively affect the generation of Li metal debris. The stripping of irregular deposits at slow rates induced thinning of the necking regions, thus increasing the risk of the formation of dead Li. We believe that our findings not only elucidate the quantitative Li growth behaviors under various electrochemical conditions but also provide important clues about the basic mechanism of abnormal Li growth that occurs during battery operation and causes premature failure of Li metal anodes. It is our hope that these fundamental studies will aid in the development of effective counter strategies to regulate the growth of Li metal and enable the use of high-energy-density Li metal anodes.

ASSOCIATED CONTENT

Supporting Information

. Videos for time-dependent geometry evolution. The Supporting Information is available free of charge on the ACS Publications website at DOI: 10.1021/acs.chemmater.8b02623.

Models used for simulation with different surface shapes, SEI layers. Shape of Li deposits after a deposition with 50 nm-thick SEI layer, and stripping from artificially made model with narrow points (PDF)

Video for time-dependent geometry evolution (AVI)
Video for time-dependent geometry evolution (AVI)
Video for time-dependent geometry evolution (AVI)
Video for time-dependent geometry evolution (AVI)

AUTHOR INFORMATION

Corresponding Author

*Tel.: +82-2-880-7088. Fax.: +82-2-885-9671. E-mail: matlgen1@snu.ac.kr (K.K.).

ORCID

Kisuk Kang: 0000-0002-8696-1886

Author Contributions

The manuscript was written through contributions of all authors. All authors have given approval to the final version of the manuscript.

Notes

The authors declare no competing financial interest.

ACKNOWLEDGMENTS

This work was supported by IBS-R006-G1 and Creative Materials Discovery Program through the National Research Foundation of Korea (NRF) funded by the Ministry of Science, ICT and Future Planning (NRF-2017M3D1A1039553). G.Y. is grateful to Byungju Lee for helpful discussions.

REFERENCES

(1) Tarascon, J. M.; Armand, M. Issues and challenges facing rechargeable lithium batteries. *Nature* **2001**, *414*, 359−367.

(2) Choi, J. W.; Aurbach, D. Promise and reality of post-lithium-ion batteries with high energy densities. *Nat. Rev. Mater.* **2016**, *1*, 16013.

(3) Li, Z.; Huang, J.; Yann Liaw, B.; Metzler, V.; Zhang, J. A review of lithium deposition in lithium-ion and lithium metal secondary batteries. *J. Power Sources* **2014**, *254*, 168−182.

(4) Zhang, K.; Lee, G.-H.; Park, M.; Li, W.; Kang, Y.-M. Recent Developments of the Lithium Metal Anode for Rechargeable Non-Aqueous Batteries. *Adv. Energy Mater.* **2016**, *6*, 1600811.

(5) Guo, Y.; Li, H.; Zhai, T. Reviving Lithium-Metal Anodes for Next-Generation High-Energy Batteries. *Adv. Mater.* **2017**, *29*, 1700007.

(6) Wood, K. N.; Noked, M.; Dasgupta, N. P. Lithium Metal Anodes: Toward an Improved Understanding of Coupled Morphological, Electrochemical, and Mechanical Behavior. *ACS Energy Lett.* **2017**, *2*, 664−672.

(7) Xu, W.; Wang, J.; Ding, F.; Chen, X.; Nasybulin, E.; Zhang, Y.; Zhang, J.-G. Lithium metal anodes for rechargeable batteries. *Energy Environ. Sci.* **2014**, *7*, 513−537.

(8) Qian, J.; Henderson, W. A.; Xu, W.; Bhattacharya, P.; Engelhard, M.; Borodin, O.; Zhang, J.-G. High rate and stable cycling of lithium metal anode. *Nat. Commun.* **2015**, *6*, 6362.

(9) Zaban, A.; Aurbach, D. Impedance spectroscopy of lithium and nickel electrodes in propylene carbonate solutions of different lithium salts A comparative study. *J. Power Sources* **1995**, *54*, 289−295.

(10) Monroe, C.; Newman, J. The Impact of Elastic Deformation on Deposition Kinetics at Lithium/Polymer Interfaces. *J. Electrochem. Soc.* **2005**, *152*, A396−A404.

(11) Chen, X.; Hou, T.-Z.; Li, B.; Yan, C.; Zhu, L.; Guan, C.; Cheng, X.-B.; Peng, H.-J.; Huang, J.-Q.; Zhang, Q. Towards stable lithium-sulfur batteries: Mechanistic insights into electrolyte decomposition on lithium metal anode. *Energy Storage Materials* **2017**, *8*, 194−201.

(12) Zu, C.; Azimi, N.; Zhang, Z.; Manthiram, A. Insight into lithium-metal anodes in lithium-sulfur batteries with a fluorinated ether electrolyte. *J. Mater. Chem. A* **2015**, *3*, 14864−14870.

(13) Yan, K.; Lee, H.-W.; Gao, T.; Zheng, G.; Yao, H.; Wang, H.; Lu, Z.; Zhou, Y.; Liang, Z.; Liu, Z.; Chu, S.; Cui, Y. Ultrathin Two-

DOI: 10.1021/acs.chemmater.8b02623
Chem. Mater. 2018, 30, 6769−6776

Dimensional Atomic Crystals as Stable Interfacial Layer for Improvement of Lithium Metal Anode. *Nano Lett.* **2014**, *14*, 6016−6022.
(14) Kazyak, E.; Wood, K. N.; Dasgupta, N. P. Improved Cycle Life and Stability of Lithium Metal Anodes through Ultrathin Atomic Layer Deposition Surface Treatments. *Chem. Mater.* **2015**, *27*, 6457−6462.
(15) Kozen, A. C.; Lin, C.-F.; Pearse, A. J.; Schroeder, M. A.; Han, X.; Hu, L.; Lee, S.-B.; Rubloff, G. W.; Noked, M. Next-Generation Lithium Metal Anode Engineering via Atomic Layer Deposition. *ACS Nano* **2015**, *9*, 5884−5892.
(16) Zheng, G.; Lee, S. W.; Liang, Z.; Lee, H.-W.; Yan, K.; Yao, H.; Wang, H.; Li, W.; Chu, S.; Cui, Y. Interconnected hollow carbon nanospheres for stable lithium metal anodes. *Nat. Nanotechnol.* **2014**, *9*, 618−623.
(17) Lee, H.; Lee, D. J.; Kim, Y.-J.; Park, J.-K.; Kim, H.-T. A simple composite protective layer coating that enhances the cycling stability of lithium metal batteries. *J. Power Sources* **2015**, *284*, 103−108.
(18) Li, N. W.; Yin, Y. X.; Yang, C. P.; Guo, Y. G. An Artificial Solid Electrolyte Interphase Layer for Stable Lithium Metal Anodes. *Adv. Mater.* **2016**, *28*, 1853−1858.
(19) Wang, X.; Hou, Y.; Zhu, Y.; Wu, Y.; Holze, R. An Aqueous Rechargeable Lithium Battery Using Coated Li Metal as Anode. *Sci. Rep.* **2013**, *3*, 1401.
(20) Lu, Y.; Tu, Z.; Archer, L. A. Stable lithium electrodeposition in liquid and nanoporous solid electrolytes. *Nat. Mater.* **2014**, *13*, 961−969.
(21) Lu, Y.; Tu, Z.; Shu, J.; Archer, L. A. Stable lithium electrodeposition in salt-reinforced electrolytes. *J. Power Sources* **2015**, *279*, 413−418.
(22) Ding, F.; Xu, W.; Graff, G. L.; Zhang, J.; Sushko, M. L.; Chen, X.; Shao, Y.; Engelhard, M. H.; Nie, Z.; Xiao, J.; Liu, X.; Sushko, P. V.; Liu, J.; Zhang, J.-G. Dendrite-Free Lithium Deposition via Self-Healing Electrostatic Shield Mechanism. *J. Am. Chem. Soc.* **2013**, *135*, 4450−4456.
(23) Wang, S.-H.; Yin, Y.-X.; Zuo, T.-T.; Dong, W.; Li, J.-Y.; Shi, J.-L.; Zhang, C.-H.; Li, N.-W.; Li, C.-J.; Guo, Y.-G. Stable Li Metal Anodes via Regulating Lithium Plating/Stripping in Vertically Aligned Microchannels. *Adv. Mater.* **2017**, *29*, 1703729.
(24) Rosso, M.; Gobron, T.; Brissot, C.; Chazalviel, J. N.; Lascaud, S. Onset of dendritic growth in lithium/polymer cells. *J. Power Sources* **2001**, *97*−*98*, 804−806.
(25) Brissot, C.; Rosso, M.; Chazalviel, J. N.; Lascaud, S. Dendritic growth mechanisms in lithium/polymer cells. *J. Power Sources* **1999**, *81*−*82*, 925−929.
(26) Chazalviel, J. N. Electrochemical aspects of the generation of ramified metallic electrodeposits. *Phys. Rev. A: At., Mol., Opt. Phys.* **1990**, *42*, 7355−7367.
(27) Rosso, M.; Chassaing, E.; Chazalviel, J. N.; Gobron, T. Onset of current-driven concentration instabilities in thin cell electrodeposition with small inter-electrode distance. *Electrochim. Acta* **2002**, *47*, 1267−1273.
(28) Sand, H. J. S., III. On the concentration at the electrodes in a solution, with special reference to the liberation of hydrogen by electrolysis of a mixture of copper sulphate and sulphuric acid. *Philos. Mag.* **1901**, *1*, 45−79.
(29) Bai, P.; Li, J.; Brushett, F. R.; Bazant, M. Z. Transition of lithium growth mechanisms in liquid electrolytes. *Energy Environ. Sci.* **2016**, *9*, 3221−3229.
(30) "COMSOL Multiphysics Reference Manual, version 5.3", COMSOL, Inc., www.comsol.com.
(31) Valøen, L. O.; Reimers, J. N. Transport Properties of LiPF6-Based Li-Ion Battery Electrolytes. *J. Electrochem. Soc.* **2005**, *152*, A882−A891.
(32) Verma, P.; Maire, P.; Novák, P. A review of the features and analyses of the solid electrolyte interphase in Li-ion batteries. *Electrochim. Acta* **2010**, *55*, 6332−6341.
(33) Peled, E. The Electrochemical Behavior of Alkali and Alkaline Earth Metals in Nonaqueous Battery Systems—The Solid Electrolyte Interphase Model. *J. Electrochem. Soc.* **1979**, *126*, 2047−2051.
(34) Moon, S.; Park, H.; Yoon, G.; Lee, M. H.; Park, K.-Y.; Kang, K. Simple and Effective Gas-Phase Doping for Lithium Metal Protection in Lithium Metal Batteries. *Chem. Mater.* **2017**, *29*, 9182−9191.
(35) Yang, C.-P.; Yin, Y.-X.; Zhang, S.-F.; Li, N.-W.; Guo, Y.-G. Accommodating lithium into 3D current collectors with a submicron skeleton towards long-life lithium metal anodes. *Nat. Commun.* **2015**, *6*, 8058.
(36) Yun, Q.; He, Y.-B.; Lv, W.; Zhao, Y.; Li, B.; Kang, F.; Yang, Q.-H. Chemical Dealloying Derived 3D Porous Current Collector for Li Metal Anodes. *Adv. Mater.* **2016**, *28*, 6932−6939.

DOI: 10.1021/acs.chemmater.8b02623
Chem. Mater. 2018, 30, 6769−6776